

# The Impact of the Quantum Data Plane Overhead on the Throughput

Jessica Illiano

University of Naples *Federico II*  
Naples, ITALY  
jessica.illiano@unina.it

Antonio Manzalini

Telecomitalia  
Turin, ITALY  
antonio.manzalini@telecomitalia.it

Angela Sara Cacciapuoti

University of Naples *Federico II*,  
Naples, ITALY  
angelasara.cacciapuoti@unina.it

Marcello Caleffi

University of Naples *Federico II*,  
Naples, ITALY  
marcello.caleffi@unina.it

## ABSTRACT

Currently, although a standard distinction between quantum data plane and quantum control plane is still missing, preliminary works specify that classical control messages operating at the granularity of individual qubits and entangled pairs are, in terms of functionalities, closer to classical packet headers than control plane messages. Thus, they have been considered as part of the quantum data plane, by contributing to its overall overhead. As a consequence, the very concept of throughput needs to be re-defined and studied within the Quantum Internet. The aim of this treatise is to shed the light on this crucial aspect. Specifically, we conduct a theoretical analysis to understand the factors determining the overhead in the quantum data plane and their reflection on the throughput. The analysis is crucial and preliminary for designing any effective quantum communication protocol. Specifically, we derive closed-form expressions of the throughput in different scenarios, and the non-linear relationship between throughput, entanglement throughput and classical bit rate is disclosed. Finally, we validate the theoretical analysis through numerical results conducted on the *IBM Q-Experience platform*.

## KEYWORDS

Quantum Internet, Quantum Networks, Quantum Communications, Entanglement, Quantum Teleportation

### ACM Reference Format:

Jessica Illiano, Angela Sara Cacciapuoti, Antonio Manzalini, and Marcello Caleffi. 2021. The Impact of the Quantum Data Plane Overhead on the

---

This work was partially supported by the project “Towards the Quantum Internet: A Multidisciplinary Effort”, University of Naples Federico II, Italy and by the PON project “S4E - Sistemi di Sicurezza e Protezione per l’Ambiente Mare”, Naples, 80126 Italy.

Jessica Illiano acknowledges support from TIM S.p.A. through the PhD scholarship. Angela Sara Cacciapuoti and Marcello Caleffi are also with *Laboratorio Nazionale di Comunicazioni Multimediali CNIT*, Naples, 80126 Italy.

---

Permission to make digital or hard copies of all or part of this work for personal or classroom use is granted without fee provided that copies are not made or distributed for profit or commercial advantage and that copies bear this notice and the full citation on the first page. Copyrights for components of this work owned by others than the author(s) must be honored. Abstracting with credit is permitted. To copy otherwise, or republish, to post on servers or to redistribute to lists, requires prior specific permission and/or a fee. Request permissions from [permissions@acm.org](mailto:permissions@acm.org).

NANOCOM '21, September 7–9, 2021, Virtual Event, Italy

© 2021 Copyright held by the owner/author(s). Publication rights licensed to ACM.

ACM ISBN 978-1-4503-8710-1/21/09...\$15.00

<https://doi.org/10.1145/3477206.3477448>

Throughput. In *The Eight Annual ACM International Conference on Nanoscale Computing and Communication (NANOCOM '21)*, September 7–9, 2021, Virtual Event, Italy. ACM, New York, NY, USA, 6 pages. <https://doi.org/10.1145/3477206.3477448>

## 1 INTRODUCTION

When it comes to the Quantum Internet [2, 5, 12], due to the different nature of the underlying physical mechanisms, it is not possible to adopt the same approaches and protocols holding in the classical networks by inference. Actually, the design of an abstract quantum network model that leads to the definition of a reference standard is still an open problem. This model has to harness the peculiarities of quantum mechanics and the intrinsic interactions between the quantum network and a classical network.

In this regard, a crucial aspect is represented by the distinction between quantum data plane and quantum control plane. In fact, the aforementioned distinction allows a more effective design of the abstract quantum network model along with its functionalities. Currently, a standard distinction between data and control planes is still missing, although the debate is ongoing and boiled. A preliminary work has been made in [10], where it has been specified that control information messages operating at the granularity of individual qubits and entangled pairs, such as heralding messages used for elementary link generation are, in terms of functionalities, closer to classical packet headers than control plane messages. Thus, they have been considered as part of the quantum data plane. Hence, according to this preliminary standard [10], a quantum data plane also includes the exchange of classical control information at the granularity of individual qubits and entangled pairs.

With the aforementioned discussion in mind, it is clear that this classical control information contributes to the overall overhead characterizing the quantum data plane. Hence, the very concept of throughput needs to be re-defined and studied.

The aim of this treatise is to shed the light on this crucial aspect. Specifically, we conduct a theoretical analysis to understand the factors determining the overhead in the quantum data plane and their reflection on the throughput. The analysis is crucial and preliminary for designing any effective quantum communication protocol.

In the following, we focus on the *quantum teleportation*, since it represents a concrete example of quantum communication protocol that exploits the control information messages operating at

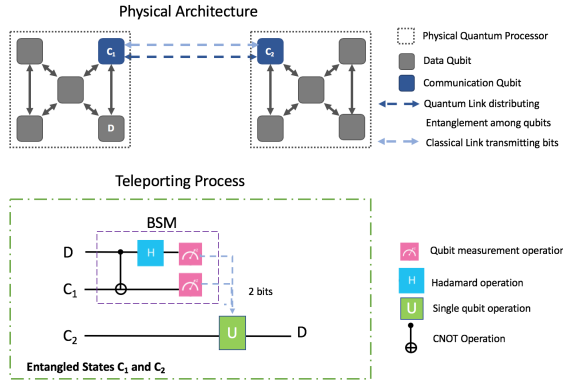


**Figure 1: Physical Network Architecture and Quantum Teleportation process.**

the granularity of individual qubits and entangled pairs [2, 5, 8]. The conducted analysis can be easily extended to other quantum communication protocols, affected by the quantum data-plane overhead.

Specifically, the quantum teleportation process [3] requires the support of the classical network for exchanging control information messages for the entanglement generation and distribution process as well as for the sharing of the classical output (2 bits as detailed in Section 2) of the Bell-State Measurement (BSM). These control information represents quantum data plane overhead.

Stemming from this, we re-define the concept of quantum throughput. Closed-form expressions of the throughput are derived in different scenarios, and the non-linear relationship between throughput, entanglement rate and classical bit rate is disclosed.

Finally, we validate the theoretical analysis through numerical results conducted on the *IBM Q-Experience platform* [7].

## 2 MODELING AND PRELIMINARIES

### 2.1 Quantum Network Architecture and Quantum Teleportation

We consider the quantum network architecture shown in Fig. 1, where quantum information must be transmitted between two quantum processors. Each quantum processor has two different subsets of qubits: *communication qubits* and *data qubits* [10]. Communication qubits are devoted to the entanglement generation and distribution process [10]. Data qubits are devoted to store and process the quantum states. Generally, the two subsets have different physical implementations, therefore a qubit cannot be used as communication qubit and as data qubit, contemporaneously. In Fig. 1, the communication qubits are denoted with the capital letter  $C$ . As explained in Sec. 3, this separation affects the communication process and the throughput.

As mentioned in the introduction, we consider the quantum teleportation as a concrete example of quantum communication protocol that exploits the control information messages operating at the granularity of individual qubits and entangled pairs.

More in detail, quantum teleportation provides an invaluable strategy for transmitting qubits without the physical transfer of

the particle storing the qubit [2]. Indeed, with just local operations, referred to as *Bell-State Measurement* (BSM), and a couple of maximally entangled qubits, referred to as *EPR pair*, shared between source and destination, quantum teleportation allows one to “transmit” an unknown quantum state [2, 5, 13].

Quantum teleportation implies the destruction of both the original qubit (encoding the quantum information to be transmitted and denoted in Fig. 1 with the capital letter  $D$ ) and the EPR member at the source, as a consequence of the BSM. Indeed, the original qubit is reconstructed at the destination once the output of the BSM at the source – 2 classical bits – is received through a classical link. These bits are used at the destination to choose, among 4 possible operations, the unique operation  $U(\cdot)$  able to transform the communication qubit at the receiver, i.e.,  $C_2$  in Fig. 1, into the original quantum state  $D$ .

Furthermore, as mentioned above, the EPR pair is depleted during the teleportation and a new EPR pair must be generated and distributed between the communication qubits before a new quantum teleportation process could occur. But, at the end of the previous teleportation, the communication qubit at the destination is storing the reconstructed quantum state  $D$ . Hence, before generating/distributing a new EPR pair involving the same communication qubits, the transmitted quantum state must be moved out of the communication qubit at the receiver through a *swap operation*<sup>1</sup>.

### 2.2 Preliminaries

In the following, we collect some definitions that will be used through the paper.

As described in Sec. 2.1, without a successful entanglement generation and distribution process, the teleportation process cannot take place. Such an entanglement generation and distribution process can be implemented through different strategies and architectures [3, 10]. In particular, the entanglement may be generated locally at one node, at both nodes or at mid-point and then distributed [3, 10].

The control messages needed in this process contributes to the overhead of the quantum data plane. To quantify such an overhead, the considered entanglement generation and distribution mechanism<sup>2</sup> has to be specified. In order to abstract from the particulars of the adopted entanglement generation and distribution process, we introduce the general parameter  $\mathcal{T}_e$ , denoting the average time needed for generating and distributing an EPR pair between the source and the destination, by including the time to exchange the required control messages. The abstraction from the particulars is very common in literature, since it leads to tractable mathematical analysis without any loss in generality.

Furthermore,  $\mathcal{T}_e$  depends on several factors, including the adopted qubit technology, the distance between source and destination, noise phenomena e.g., quantum decoherence [1, 13] [4]. In this regard,  $\mathcal{T}_e$  may depend on the adopted noise counteractions, such

<sup>1</sup>Due to the no-cloning theorem, the transmitted quantum state can not be simply copied into a data qubit. Hence, a swap operation [13], i.e., a sequence of 3 CNOTs, is necessary to “move” the transmitted state into a data qubit.

<sup>2</sup>If the entanglement is generated at source, one of the two entangled particles is sent to the destination node. The latter has to communicate, for example with an ACK, whether the particle has been received correctly or not. Only in the affirmative case the teleportation can have place. Several protocols can be designed in order to properly establish the entanglement between source and destination.

as entanglement distillation [13]. In the developed analysis and in the numerical evaluation section, we analyze and discuss these dependencies.

Stemming from the aforementioned discussion, we introduce the following definition.

**Definition 1.**  $\Gamma_e \triangleq \frac{1}{T_e}$  denotes the entanglement throughput, which can be determined as the inverse of the average time  $T_e$ .

**Definition 2.**  $\mathcal{T}_{BSM}$  denotes the average time to perform a BSM at the source and the unique operation  $U(\cdot)$ , whereas  $\mathcal{T}_{SW}$  denotes the average time to perform a swap operation at the destination.

**Definition 3.**  $\mathcal{R}_b$  denotes the bit rate characterizing the considered classical communication channel between the source and the destination, whereas  $\mathcal{T}_c$  denotes the communication delay for receiving, at the destination, the output of the BSM performed at the source.

Both  $\mathcal{T}_{BSM}$  and  $\mathcal{T}_{SW}$  depend on the particulars of the adopted qubit technology. Furthermore, in an heterogeneous hardware scenario, such times may vary among the network nodes.  $\mathcal{T}_c$  depends on the distance between source and destination, propagation characteristics of the considered medium (e.g., free-space, fiber, etc.), the particulars of the adopted classical communication strategy.

**Definition 4.**  $\Gamma$  denotes the teleporting throughput  $\Gamma$ , i.e., the effective number of qubits successfully delivered through a quantum communication link in the time unit.

### 3 THROUGHPUT ANALYSIS

Here, first in Sec. 3.1 we develop the theoretical analysis by assuming that each quantum processor has only one communication qubit, as depicted in Fig. 1. Then, in Sec. 3.2 we generalize the analysis by considering  $N$  communication qubits for each processor, as depicted in Fig. 2. Finally, in Sec. 3.3, we extend the analysis to quantum repeater network architectures.

#### 3.1 Single Communication Qubit

**PROPOSITION 1.** *The teleportation throughput  $\Gamma$  is given by:*

$$\Gamma = \frac{\mathcal{R}_b \Gamma_e}{2\Gamma_e + \mathcal{R}_b + \mathcal{R}_b \Gamma_e (\mathcal{T}_{SW} + \mathcal{T}_{BSM} + \mathcal{T}_c)} \quad (1)$$

with the parameters in (1) defined in Sec. 2.2.

**PROOF.** By accounting for Sec. 2.1 and Fig. 1, the average time  $\mathcal{T}_{telep}$  needed to perform a quantum teleportation is:

$$\mathcal{T}_{telep} = \mathcal{T}_e + \mathcal{T}_{BSM} + \frac{2}{\mathcal{R}_b} + \mathcal{T}_c \quad (2)$$

where  $\frac{2}{\mathcal{R}_b} + \mathcal{T}_c$  accounts for the average time occurred between the starting of BSM-output transmission at the source and the ending of BSM-output reception at the destination. This time, as mentioned in Sec. 2.2 concurs to the overall data plane overhead. After completion of the teleportation, communication qubit  $C_2$  at destination stores the transmitted quantum state. Hence, before starting a new teleportation process, the transmitted quantum state needs to be “moved out” of  $C_2$  with a SWAP operation so that a new EPR pair can be generated/distributed. Hence, the average time between two consecutive teleportation processes is  $\mathcal{T} = \mathcal{T}_{telep} + \mathcal{T}_{SW}$ .

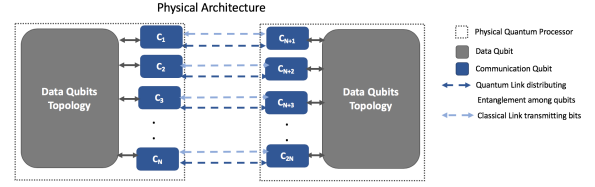


**Figure 2: Pictorial Representation of Multiple Communication Qubits.**

By substituting (2) in the above equation, after some algebraic manipulations, the proof follows.  $\square$

Equation (1) reveals the non-linear dependence of the throughput from the quantum data plane overhead. Furthermore, some considerations can be made. Specifically, if  $\Gamma_e$  goes to zero also the throughput goes to zero. This is trivial because without entanglement generation and distribution the connectivity is forbidden. As  $\mathcal{T}_e$  goes to zero, that is  $\Gamma_e \rightarrow \infty$ , the throughput is strongly influenced by the classical network QoS:

$$\Gamma \xrightarrow{\Gamma_e \rightarrow \infty} \frac{1}{\frac{2}{\mathcal{R}_b} + \mathcal{T}_{BSM} + \mathcal{T}_{SW} + \mathcal{T}_c} \quad (3)$$

In this analysis we assume that there’s always a data qubit available for the swapping operation. Otherwise,  $\mathcal{T}_{SW}$  is not only given by the quantum gate time, but there’s eventually an additional waiting time.  $\mathcal{R}_b$  and  $\mathcal{T}_c$  take value in a range that can vary widely with the physical medium and the communication protocol adopted. Through  $\mathcal{R}_b$  and  $\mathcal{T}_c$  the classical network has a direct the impact on the teleporting throughput. We determine from Prop. 1 the entity of this impact.

**COROLLARY 1.** *The  $\Gamma$  is upper-bounded as follows:*

$$\Gamma < \frac{\mathcal{R}_b}{2} \quad (4)$$

**PROOF.** The proof follows directly from (1), by accounting for the positiveness of the involved parameters.  $\square$

**Insight 1.** The result of Cor. 1 proves that  $\Gamma$  is limited by (half) the bit rate of a classical link. Furthermore, by reasoning as in Cor. 1, from (1) it results:

$$\Gamma < \Gamma_e. \quad (5)$$

Hence, the  $\Gamma$  cannot exceed the entanglement throughput  $\Gamma_e$ . As indicated in Sec. 2.2,  $\Gamma_e$  accounts for the data plane overhead related to the entanglement generation and distribution process, that is a limiting factor for the teleporting throughput. A tighter bound could be derived in the asymptotic regime, i.e., when  $\mathcal{R}_b \rightarrow \infty$ . Specifically, from (1) it results:

$$\Gamma \xrightarrow{\mathcal{R}_b \rightarrow \infty} \frac{\Gamma_e}{1 + \Gamma_e (\mathcal{T}_{SW} + \mathcal{T}_{BSM} + \mathcal{T}_c)} < \Gamma_e \quad (6)$$

Thus, even if the classical communication link is characterized by an hypothetical infinite bit rate,  $\Gamma$  is bounded by  $\Gamma_e$ .

### 3.2 Multiple Communication Qubits

When a quantum processor is equipped with only one communication qubit, it cannot simultaneously generate and distribute more than one EPR pairs [10]. If  $N_D$  is the number of data qubits, we consider quantum processors such that  $N < N_D$ .

PROPOSITION 2. *The teleportation throughput is equal to:*

$$\Gamma^N = \frac{N\Gamma\mathcal{R}_b}{\mathcal{R}_b + 2(N-1)\Gamma} \quad (7)$$

where  $\Gamma$  is the throughput when only one communication qubit is available and it has been derived in (1).

PROOF. When  $N$  qubits are devoted to the communication task at each processor,  $N$  teleportation processes can be performed simultaneously in the hypothesis of perfect synchronization<sup>3</sup>. Hence, the average time is given by  $\mathcal{T}_{\text{telep}}^N = \mathcal{T}_e + \mathcal{T}_{\text{BSM}} + \frac{2N}{\mathcal{R}_b} + \mathcal{T}_c$ , where  $\frac{2N}{\mathcal{R}_b} + \mathcal{T}_c$  accounts for the average time occurred between the starting of the transmission of  $N$  BSM-outputs at the source and the ending of the reception of the BSM-outputs at the destination. This time, as mentioned in Sec. 2.2 concurs to the overall data plane overhead. Then, the  $N$  communication qubits must be set free with  $N$  swap operations performed in batch. By accounting for the above, the average time between two consecutive teleportation processes is  $\mathcal{T} = \mathcal{T}_{\text{telep}}^N + \mathcal{T}_{\text{SW}}$ . By dividing the above equation for the number  $N$  of transmitted qubits and by inverting it, it results:

$$\Gamma^N = \frac{N\mathcal{R}_b\Gamma_e}{2N\Gamma_e + \mathcal{R}_b + \mathcal{R}_b\Gamma_e(\mathcal{T}_{\text{SW}} + \mathcal{T}_{\text{BSM}} + \mathcal{T}_c)} \quad (8)$$

From (8), by accounting for (1), after some algebraic manipulations, the proof follows.  $\square$

COROLLARY 2. *The teleportation throughput  $\Gamma^N$  increases with the number  $N$  of communication qubits available at each processor, i.e.:*

$$\Gamma^{N_1} > \Gamma^{N_2}, \quad \text{with } N_1 > N_2 \quad (9)$$

PROOF. We prove the corollary with a *reductio ad absurdum* by supposing that  $\exists N_1, N_2$ , with  $N_1 > N_2 : \Gamma^{N_1} \leq \Gamma^{N_2}$ . By substituting (7) in the above inequality, it results:

$$\frac{N_1\Gamma\mathcal{R}_b}{\mathcal{R}_b + 2(N_1-1)\Gamma} \leq \frac{N_2\Gamma\mathcal{R}_b}{\mathcal{R}_b + 2(N_2-1)\Gamma} \quad (10)$$

After some algebraic manipulations, (10) is equivalent to  $(N_1 - N_2)(\mathcal{R}_b - 2\Gamma) \leq 0$ , which constitutes a *reductio ad absurdum* since  $N_1 > N_2$  and  $\mathcal{R}_b > 2\Gamma$  from Cor. 1.  $\square$

COROLLARY 3. *The teleportation throughput  $\Gamma^N$  is upper-bounded as follows:*

$$\Gamma^N < N\Gamma < \frac{N}{2}\mathcal{R}_b \quad (11)$$

PROOF. The proof follows directly from (7), by accounting for the positiveness of the involved parameters and for (??).  $\square$

<sup>3</sup>The perfect synchronization of  $N$  teleportation processes may be managed using the classical network, designing a proper protocol for this purpose is a topic that needs further study and is beyond the scope of this paper

**Insight 2.** Cor. 3 proves that  $\Gamma^N$ , when  $N$  communication qubits are reserved at each processor, is limited by  $N/2$  times the classical bit rate. Indeed, Cor. 3 can be equivalently re-written, by accounting for the inequality (5), as:

$$\Gamma^N < N\Gamma < N\Gamma_e. \quad (12)$$

Consequently,  $\Gamma^N$  is still bounded by the entanglement throughput, specifically it cannot be greater than the rate at which  $N$  EPR pairs are contemporaneously generated and distributed. A tighter bound could be derived in the asymptotic regime, i.e., when  $\mathcal{R}_b \rightarrow \infty$ , by exploiting (6) and (7):

$$\Gamma^N \xrightarrow{\mathcal{R}_b \rightarrow \infty} \frac{N\Gamma_e}{1 + \Gamma_e(\mathcal{T}_{\text{SW}} + \mathcal{T}_{\text{BSM}} + \mathcal{T}_c)} < N\Gamma_e \quad (13)$$

Thus, even if  $\mathcal{R}_b \rightarrow \infty$ ,  $N\Gamma_e$  is a tight bound for  $\Gamma^N$ .

**Remark.**  $\Gamma$  and  $\Gamma^N$  are affected by the quantum data plane overhead. Furthermore, they are subjected to the noise effects via  $\Gamma_e$ . However, the noise does not affect only the teleporting throughput. Specifically, teleportation consists of a sequence of operations on a quantum state. The imperfections of such operations and the decoherence affect the fidelity of the reconstructed qubit at destination. This constitutes another challenge from a communication perspective. We analyze this effects in Sec. 4.2.

### 3.3 Quantum Repeater Architecture

The previous analysis can be extended by considering a more complex architecture shown in Fig. 3, relying on quantum repeaters [11]. Here, due to the space limit, we limit our attention to single communication qubit available at each node. The quantum repeater are intermediate node between the source and the destination implementing the physical process called *entanglement swapping* over its communication qubits. The result of this procedure is the end-to-end entanglement between  $C_1$  and  $C_{N+1}$ . Similarly to the definition given in Sec. 2.1, we denote with  $\Gamma_{er} = \frac{1}{\mathcal{T}_{er}}$  the end-to-end entanglement throughput. As  $\Gamma_e$  introduced in Sec. 2.2, this parameter accounts for the quantum data plane overhead.

PROPOSITION 3. *The teleportation throughput  $\Gamma_r$  in an architecture characterized by  $H$  quantum repeater is given by:*

$$\Gamma_r = \frac{\min_{i=0,\dots,H} \mathcal{R}_{b_i} \Gamma_{er}}{2\Gamma_{er} + \min_{i=0,\dots,H} \mathcal{R}_{b_i} + \min_{i=0,\dots,H} \mathcal{R}_{b_i} \Gamma_{er} [\mathcal{T}_{\text{SW}} + \mathcal{T}_{\text{BSM}} + \sum_{i=0}^H \mathcal{T}_{c_i}]}, \quad (14)$$

where  $\{\mathcal{R}_{b_i}\}$  and  $\{\mathcal{T}_{c_i}\}$  denote the bit-rate and the communication delay of each link, respectively.

PROOF. If  $H$  is the number of quantum repeaters involved in the teleportation process between source and destination the average time  $\mathcal{T}_{\text{telep}}$  needed to accomplish the procedure is:

$$\mathcal{T}_{\text{telep}} = \mathcal{T}_{er} + \mathcal{T}_{\text{BSM}} + \frac{2}{\min_{i=0,\dots,H} \mathcal{R}_{b_i}} + \sum_{i=0}^H \mathcal{T}_{c_i}, \quad (15)$$

where we exploited the deferred measurement process [13]. With the redefined parameters the proof follows similarly as in Prop. 1.  $\square$

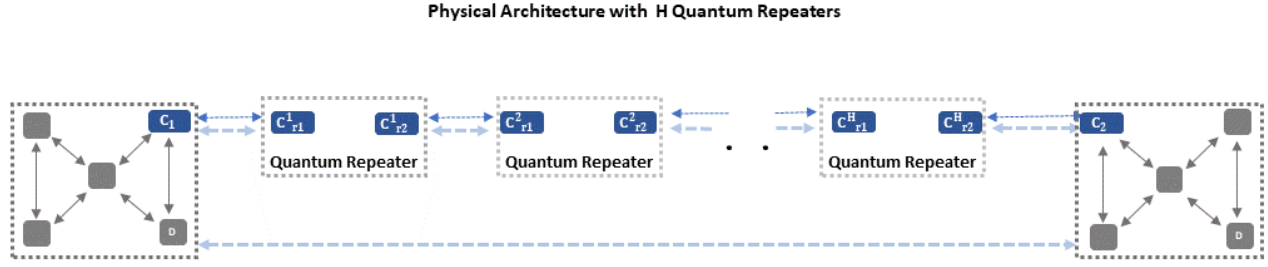


**Figure 3: Schematic Representation of Quantum Repeater Architecture**

From Prop.3, similar considerations made in the previous section, can be drawn.

## 4 PERFORMANCE ANALYSIS

Here, we first analyze in Sec. 4.1 the impact of the different parameters on the throughput  $\Gamma$  through Monte-Carlo simulations, in agreement with the theoretical analysis developed in Sec. 3. Then, we assess in Sec. 4.2 the noise effects on the teleportation process, by conducting an experiment with a real quantum computer through the *IBM Q-Experience*.

### 4.1 Throughput

We consider a quantum network architecture operating through atoms in optical cavities [4]. This choice is motivated by the availability of experimental results allowing us to properly set all the parameters, but the developed analysis continues to hold regardless of the specificity of the network architecture and parameter setting.

In Fig. 4, we show  $\Gamma$  given in (1) as a function of the link length for different values of the  $\mathcal{T}_{\text{BSM}}$ . Specifically,  $\mathcal{T}_{\text{BSM}}$  ranges from  $4\mu\text{s}$  to  $0.1\text{ms}$ . This choice is reasonable, since CNOT times of  $2\mu\text{s}$  have been recently reported in [15]. Furthermore, given that a SWAP operation consists of three CNOTs, we set  $\mathcal{T}_{\text{SW}} = 3\mathcal{T}_{\text{BSM}}$ . Finally,  $\mathcal{R}_b = 10^8\text{bit/s}$  and all the parameters ruling the entanglement generation and distribution have been set in agreement with experimental results [9, 14]. We note that, as expected,  $\Gamma$  decreases with the distance between source and destination, since both the entanglement throughput  $\Gamma_e$  and the communication delay  $\mathcal{T}_c$  are affected by such a distance. This behavior is in agreement with (1). Furthermore, according to Cor. 1 and Ins. 1,  $\Gamma$  never exceeds  $\mathcal{R}_b/2$  ( $5 \cdot 10^7\text{bit/s}$  in our simulation set) as well as  $\Gamma_e$ . Then, in Fig. 4, we consider the effects of the decoherence on  $\Gamma$  as well. Specifically, we set the coherence time ranging roughly from  $10^{-4}$  to  $10^{-1}$  seconds in agreement with literature [6]. We note that, for each considered coherence time value, it is possible to identify a distance threshold, represented in the figure with a vertical dotted line. Specifically, for any link length greater than the threshold, the throughput drops to zero, since the time required for a teleportation exceeds the qubit coherence time. This behavior is theoretically expected since, when the coherence time is exceeded, the entanglement generation and distribution rate goes to zero and so does  $\Gamma$ , in agreement with (1).

Finally, in Fig. 5, we extend the analysis to Sec. 3.2. Specifically, we report  $\Gamma^N$  as function of the number  $N$  of communication qubits.

In agreement with the theoretical analysis,  $\Gamma^N$  increases with  $N$  and it does not exceed  $NT$ .

### 4.2 IBM Q-Experience

The IBM Q-Experience does not allow us yet to account for the channel effects within the entanglement distribution, and the adopted qubit technology is based on transmons. Nevertheless, the experiment provides us useful qualitative insights, from a communication engineering perspective, about the noise affecting the teleportation process as a result of imperfect quantum gates both at the source and the destination as well as resulting from decoherence effects. Specifically, for the quantum circuit depicted in Fig. 1, we perform over 5 millions tomography experiments using the 5-qubits IBM Tenerife *ibmqx4* quantum processor. In Fig. 6, we show the density plot of the joint PDF of the *Bloch* coordinates of the teleported quantum state when  $|0\rangle$  is the original quantum state. In absence of noise, the teleported state would coincide with the original state  $|0\rangle$ , and it will be placed at coordinates  $(0, 0, 1)$  (green dot). However, quantum noise arises during the teleportation as a consequence of several factors: i) imperfect entanglement generation, ii) imperfect quantum gates, and iii) decoherence effects. As a consequence, the teleported state differs from the original state  $|0\rangle$ , and it is not pure anymore, being transformed in a mixed one.

## 5 CONCLUSIONS

In this treatise, we analyzed the impact of the quantum data plane overhead on the throughput achievable in a quantum network. Specifically, we conducted a theoretical analysis to understand the factors determining the overhead in the quantum data plane and their reflection on the throughput. We derived closed-form expressions of the throughput in different scenarios, and the non-linear relationship between throughput, entanglement throughput and classical bit rate have been disclosed.

## REFERENCES

- [1] Angela Sara Cacciapuoti and Marcello Caleffi. 2019. Toward the Quantum Internet: A Directional-dependent Noise Model for Quantum Signal Processing. In *ICASSP 2019 - 2019 IEEE International Conference on Acoustics, Speech and Signal Processing (ICASSP)*. 7978–7982. <https://doi.org/10.1109/ICASSP.2019.8683195>
- [2] Angela Sara Cacciapuoti, Marcello Caleffi, Francesco Tafuri, Francesco Saverio Cataliotti, Stefano Gherardini, and Giuseppe Bianchi. 2020. Quantum Internet: Networking Challenges in Distributed Quantum Computing. *IEEE Network* 34, 1 (2020), 137–143. <https://doi.org/10.1109/MNET.001.1900092>

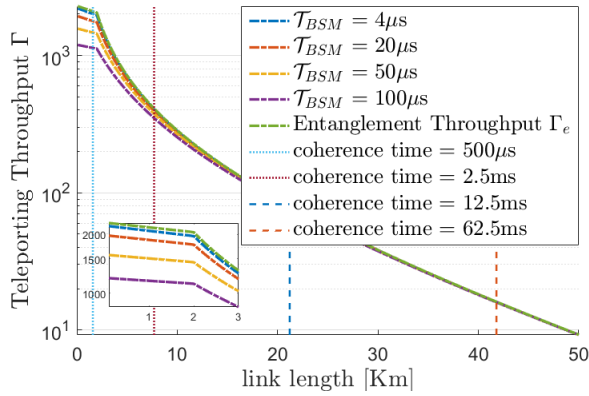


Figure 4:  $\Gamma$  vs Coherence Time as a function of the link length for different values of  $\mathcal{T}_{BSM}$ . Logarithmic scale for y axis.

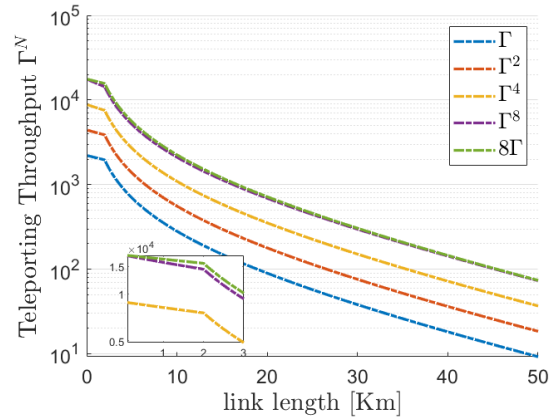


Figure 5:  $\Gamma^N$  as a function of the link length for different values of the number  $N$  of communication qubits. Logarithmic scale for y axis.

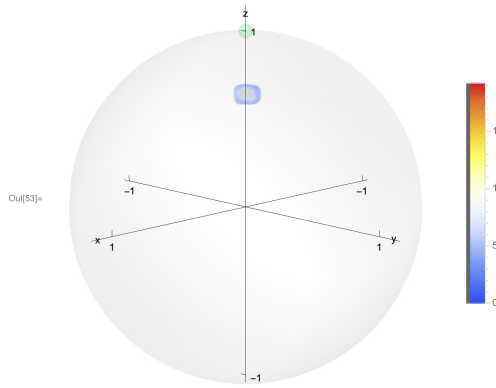


Figure 6: Bloch sphere representation of the quantum state  $|0\rangle$  teleported within IBM Tenerife *ibmqx4* quantum processor.

Between Widely Separated Atoms. 337, 6090 (2012), 72–75. <https://doi.org/10.1126/science.1221856>

- [10] Wojciech Kozłowski, Stephanie Wehner, RV Meter, Bruno Rijsman, Angela Sara Cacciapuoti, and Marcello Caleffi. 2020. Architectural principles for a quantum internet. *Internet Engineering Task Force, Internet-Draft draft-irtfqiig-principles-03* (2020).
- [11] R. Van Meter and J. Touch. 2013. Designing quantum repeater networks. *IEEE Communications Magazine* 51, 8 (2013), 64–71.
- [12] Hung Viet Nguyen, Zunaira Babar, Dimitrios Alanis, Panagiotis Botsinis, Daryus Chandra, Mohd Azri Mohd Izhar, Soon Xin Ng, and Lajos Hanzo. 2017. Towards the Quantum Internet: Generalised Quantum Network Coding for Large-Scale Quantum Communication Networks. *IEEE Access* 5 (2017), 17288–17308. <https://doi.org/10.1109/ACCESS.2017.2738781>
- [13] Michael A. Nielsen and Isaac L. Chuang. 2011. *Quantum Computation and Quantum Information: 10th Edition*. Cambridge University Press.
- [14] Manuel Uphoff, Manuel Brekenfeld, Gerhard Rempe, et al. 2016. An integrated quantum repeater at telecom wavelength with single atoms in optical fiber cavities. *Applied Physics B* 122, 3 (10 Mar 2016), 46.
- [15] Stephan Welte, Bastian Hacker, et al. 2018. Photon-Mediated Quantum Gate between Two Neutral Atoms in an Optical Cavity. *Phys. Rev. X* 8 (Feb 2018), 11. Issue 1.

- [3] Angela Sara Cacciapuoti, Marcello Caleffi, Rodney Van Meter, and Lajos Hanzo. 2020. When Entanglement Meets Classical Communications: Quantum Teleportation for the Quantum Internet. *IEEE Transactions on Communications* 68, 6 (2020), 3808–3833. <https://doi.org/10.1109/TCOMM.2020.2978071>
- [4] Marcello Caleffi. 2017. Optimal Routing for Quantum Networks. *IEEE Access* 5 (2017), 22299–22312. <https://doi.org/10.1109/ACCESS.2017.2763325>
- [5] Marcello Caleffi, Angela Sara Cacciapuoti, and Giuseppe Bianchi. 2018. Quantum Internet: From Communication to Distributed Computing!. In *Proc. 5th ACM Int. Conf. Nanoscale Comput. Commun.* Article 3. <https://doi.org/10.1145/3233188.3233224>
- [6] C. Deutsch, F. Ramirez-Martinez, C. Lacroûte, F. Reinhard, T. Schneider, J. N. Fuchs, F. Piéchon, F. Laloë, J. Reichel, and P. Rosenbusch. 2010. Spin Self-Rephasing and Very Long Coherence Times in a Trapped Atomic Ensemble. *Phys. Rev. Lett.* 105 (Jul 2010), 020401. Issue 2. <https://doi.org/10.1103/PhysRevLett.105.020401>
- [7] Davide Ferrari and Michele Amoretti. 2018. Efficient and effective quantum compiling for entanglement-based machine learning on IBM Q devices. *International Journal of Quantum Information* 16, 08 (2018), 1840006. <https://doi.org/10.1142/S0219749918400063>
- [8] Laszlo Gyongyosi, Sandor Imre, and Hung Viet Nguyen. 2018. A Survey on Quantum Channel Capacities. *IEEE Communications Surveys Tutorials* 20, 2 (2018), 1149–1205. <https://doi.org/10.1109/COMST.2017.2786748>
- [9] Julian Hofmann, Michael Krug, Norbert Ortgel, Lea Gérard, Markus Weber, Wenjamin Rosenfeld, and Harald Weinfurter. 2012. Heralded Entanglement